Journal of Electronic Materials
https://doi.org/10.1007/s11664-024-11404-2

28TH INTERNATIONAL CONFERENCE ON NUCLEAR TRACKS AND RADIATION MEASUREMENTS

Synthesis and Characterization of Sn-Doped CuO Thin Films for Gas Sensor Toward H_2S Gas Sensing

Jyoti[1] · **Rajesh Kumar**[1] · **Ashok Kumar**[2]

Received: 15 March 2024 / Accepted: 21 August 2024

Abstract
In this work, thin films of CuO doped with 3% $SnCl_2$ (0.97 g CuO-0.03 g $SnCl_2$) were deposited on glass substrates using a sol–gel spin coating technique. The deposited thin films were annealed in a muffle furnace at 400°C for 2 h. UV–visible spectroscopy, a two-probe setup, and x-ray diffraction were utilized to analyze the optical, electrical, and structural properties, respectively. The optical bandgap of the doped films was identified within the range of 3.7–3.83 eV. Electrical investigation performed by the two-probe setup revealed that the prepared samples were ohmic in nature. It was found that the resistivity of the samples varied from 11.86 Ω·m to 6.04 Ω·m as the thickness of films increased from 165 nm to 570 nm. The gas-sensing properties of the prepared films were assessed at different operational temperatures and for varying concentrations of hydrogen sulfide gas. From the obtained data, it was observed that $SnCl_2$-doped CuO thin films show excellent response toward H_2S gas at room temperature.

Keywords Doped thin films · sol–gel spin coating · XRD · UV spectroscopy · H_2S sensor

Introduction

Gas sensors play a crucial role in detecting and monitoring various gases in different environments, ranging from industrial applications to environmental monitoring. Among the multitude of gases of interest, hydrogen sulfide (H_2S) has garnered significant attention due to its toxic and corrosive nature. Because of its toxic nature, high flammability, and rotten egg-like smell, H_2S gas is easily recognized. This gas is very dangerous due to its corrosive and explosive nature.[1] When hydrogen sulfide gas comes into contact with water, an acidic solution forms which can corrode pipelines and may result in structural failure.[2,3] The main source of H_2S gas production is the decay of organic matter such as human and animal waste by anaerobic digestion. Other sources of this poisonous gas include paper mills, oil-field and power stations, tanneries, water sewage, and food processing.[4,5] A number of studies have revealed the harmful effects of H_2S on human health and environmental quality. Continuous exposure to low concentrations of H_2S gas can cause infection in the eyes and throat, and just a few tens of parts per million of this gas may result in death.[6] Therefore, it is very important to monitor its concentration for safety applications. The detection of H_2S gas is essential in industries such as petrochemicals, mining, and wastewater treatment, where its presence can pose severe health hazards and environmental concerns. As a result, the development of efficient and selective gas sensing materials is of paramount importance.

Methods that are effective for the detection of H_2S gas include fluorescent probe,[7] gas chromatography,[8] and chemical methods.[9] However, due to their complex detection processes and high cost, there is vast demand for simple and portable gas sensors. For both domestic and industrial applications, the development of H_2S gas sensors with fast response, shorter recovery time, long repeatability, low operating temperature, and high sensitivity/stability is critical. Recently, metal oxides have garnered considerable attention in gas sensing applications because of their low cost, simple fabrication, portability,

✉ Jyoti
jyotisheoran1r3@gmail.com

[1] Department of Physics, Lovely Professional University, Phagwara, Punjab 144411, India

[2] Department of Physics, Deenbandhu Chhotu Ram University of Science and Technology, Murthal, Sonipat, Haryana 131039, India

Published online: 17 September 2024

and compatibility.[10–14] These metal oxide semiconductors are categorized into two types on the basis of their charge carriers, i.e. *p*-type (CuO, Cr_2O_3, NiO, and Mn_3O_4)[15–17] and *n*-type (WO_3, TiO_2, In_2O_3, and SnO_2).[18–21]

Among these various semiconductors, *p*-type copper oxide semiconductors are widely used in gas detection, as they exhibit good response toward gases such as ozone, CO, and H_2S. CuO thin films achieve appreciable gas sensing response due to changes in resistance that reflect changing environmental conditions. CuO is an exceptional promoter of H_2S sensing owing to its conversion from *p*-type semiconducting CuO to CuS. This conversion of CuO makes it a degenerate semiconductor due to ion vacancies (Cu or S).[22–25] Copper oxide (CuO), a well-known semiconductor with a range of electronic and optical properties, has garnered attention in recent years for its potential as a gas sensing material. However, to optimize its sensing performance, researchers have explored the incorporation of dopants to enhance its gas-sensing properties. Tin (Sn) doping, in particular, has shown promise due to its ability to modify the crystal structure, electronic properties, and surface chemistry of CuO thin films, consequently influencing their gas sensing behavior.

In this work, Sn-doped CuO thin films were prepared using a sol–gel spin coating technique. The article focuses on the synthesis and characterization of Sn-doped CuO thin films for their application as gas sensors toward H_2S gas sensing. The integration of Sn into the CuO matrix is anticipated to induce structural changes that could affect the sensor's selectivity, sensitivity, and response time. Furthermore, investigating the interaction between the Sn-doped CuO thin films and H_2S gas will provide insights into the underlying sensing mechanism.

This study presents a comprehensive investigation of the synthesis process, structural analysis, and gas sensing performance of Sn-doped CuO thin films. By systematically characterizing the properties of these films and evaluating their gas sensing behavior, we aim to contribute to the understanding of how Sn doping influences the sensing capabilities of CuO-based gas sensors. This research has the potential to advance the development of high-performance gas sensors tailored for H_2S detection, with applications ranging from industrial safety to environmental monitoring. The characterization of these films was conducted using a two-probe setup, an ultraviolet (UV) spectrometer, and the x-ray diffraction (XRD) technique. The synthesized films were employed to measure their response to H_2S gas across various concentrations and operating temperatures. Among the films that were prepared, the highest response was identified in films with a thickness of 165 nm.

Experimental Details

Chemicals

All chemicals used to synthesize Sn-doped CuO thin film were of analytical grade. Tin(II) chloride ($SnCl_2$), copper acetate monohydrate (Cu $(CO_2CH_3)_2H_2O$), polyethylene glycol ($C_{2n}H_{4n+2}O_{n+1}$), isopropanol [$(CH_3)_2CHOH$], and diethanolamine ($C_4H_{11}NO_2$) were all obtained from Sigma-Aldrich (99% purity) and used as received, with no further purification.

Preparation of Sn-Doped CuO Thin Film

To create a sol with a 0.75 molar concentration, we dissolved 0.0225 g of $SnCl_2$ and 0.7275 g of copper acetate monohydrate into 9 mL of isopropanol. In this solution, we used 0.5 mL of diethanolamine as a dissolving agent and 0.5 mL of polyethylene glycol as a stabilizing agent. The solution was then kept at room temperature and stirred for 5 h until a dark blue transparent solution formed. Two drops of this solution were placed on a glass substrate positioned in a spin coater. By applying a double spinning program, a thin layer of the solution was evenly spread, and this process was carried out five times to achieve the desired film thickness. After each deposition, the sample was heated on a hot plate at 250°C for 5 min. Four samples were prepared, with the spinning speed ranging from 1500 rpm to 3000 rpm, to observe the effects of different spinning speeds. After the final deposition, these samples were placed in a muffle furnace and annealed at 400°C for 2 h to facilitate recrystallization. The synthesized samples are designated herein as 0.75MD1 for 3000 rpm, 0.75MD2 for 2500 rpm, 0.75MD3 for 2000 rpm, and 0.75MD4 for 1500 rpm for discussion.

Characterization Techniques

A UV spectrometer was employed to investigate the bandgap within the prepared samples, shedding light on their electronic properties. In addition, XRD analysis played a crucial role in revealing details about the crystalline nature, showing both the crystallite size and crystallinity of the samples. For electrical characterization, a two-probe configuration was selected, using a silver metal contact arrangement. This arrangement facilitated the measurement of essential parameters including the current–voltage (*I–V*) characteristics, resistivity, and conductivity of the sample. The metallic contact ensured accurate readings and a comprehensive understanding of the sample's electrical behavior, contributing to a holistic analysis of its physical and electronic properties.

The weight difference method was employed to quantify the thickness of the samples, as follows:

$$t = \left(W_2 - W_1\right)/(\rho * A), \tag{1}$$

where t is the thickness of the sample, W_1 is the weight of the sample before the deposition of layers, W_2 is the weight of the sample after the deposition of layers, A is the area of the sample, and ρ is the density of copper oxide.

Results and Discussion

XRD Analysis

XRD was used to evaluate the crystalline features including average size, lattice, structure, orientation, strain, and phase in the synthesized samples, providing essential details. Figure 1 depicts the XRD patterns of tin-doped CuO thin films. Analysis of the graphs reveals that the resulting films possess a polycrystalline structure. In the XRD pattern, distinctive peak positions are observed at 29.69°, 38.69°, 44.82°, 64.97°, and 77.89°, coinciding with the values specified by JCPDS card no. 89-5899. This correspondence confirms the crystalline nature of the films and their specific crystallographic phases.

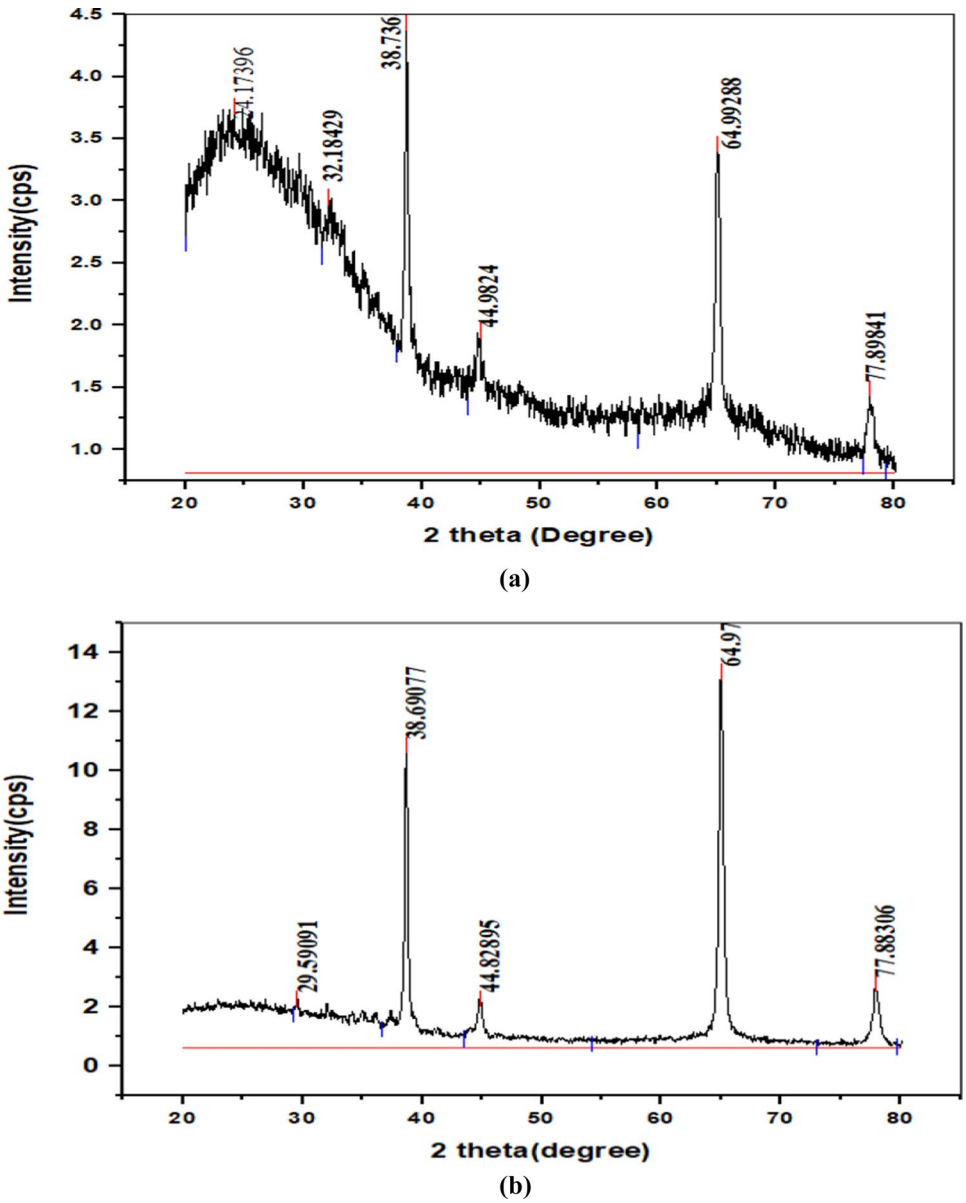

Fig. 1 XRD pattern of Sn-doped CuO thin films: (a) sample 0.75MD1 with thickness of 337 nm and (b) sample 0.75MD2 with thickness of 461 nm.

The identified peaks correspond to specific crystal planes and orientations within the material. This characterization underscores the film's well-defined crystallinity and provides insights into its structural properties.

The Debye–Scherrer equation was used to determine the size of the crystallites (D) of the synthesized materials.[26]

$$D = \frac{K\lambda}{\beta \cos\theta}, \tag{2}$$

where D represents the crystallite size of the nanoparticles, k stands for the Scherrer constant ($k = 0.89$), λ signifies the wavelength of the x-ray source (Cu-Kα) ($\lambda = 1.542$ Å), β represents the full width at half maximum (FWHM) in radians, and θ is the diffraction angle.

Crystallite sizes of 14.32 nm and 16.28 nm were determined for samples 0.75MD2 and 0.75MD3, respectively. This trend indicates that as the sample thickness increases, the crystallite size also increases. This phenomenon contributes to the enhancement of crystal imperfections, leading to improved structural properties. These findings are consistent with the results reported by Shaaban et al.[27]

Optical Properties

The optical properties of the Sn-doped CuO thin film were examined using UV–Vis spectroscopy. The energy bandgap values of the prepared CuO thin films doped with 3% Sn impacted by crystallite size and structural deformation were estimated using Tauc's relation as depicted in Eq. 3.[28,29]

$$(\alpha h\nu)^n = A(h\nu - E_g). \tag{3}$$

For a direct transition, $n = 2$, whereas for an indirect transition, $n = 1/2$. In addition, α is the absorption coefficient, $h\nu$ is the energy, and E_g is the bandgap energy.

The energy bandgap of the synthesized samples (E_g) is determined by linearly extrapolating the curve between $(\alpha h\nu)^2$ and $h\nu$ as depicted in Fig. 2. The absorption coefficient (α) plays a crucial role in measuring the quantity of light absorbed by a substance relative to its energy ($h\nu$). This method is intrinsically linked to the bandgap energy (E_g), which signifies the minimal energy required for an electron to shift from the valence band (VB) to the conduction band (CB) within a material. The bandgap energy (E_g) holds considerable significance as it governs the optical and electrical properties of the material. In optical properties, synthesized samples obey direct transition ($n = 2$), and these results are consistent with results obtained by Chackrabarti et al.[30]

The absorption coefficient (α) was derived using Lambert's law[31,32]

$$\alpha = (1/t) * \ln(1/T), \tag{4}$$

where t represents the thickness of the prepared films, and T stands for transmission.

The optical bandgap was determined within the range of 3.27–3.83 eV, illustrated in Fig. 2. This variation in the bandgap is likely attributable to the phenomenon whereby more photons are absorbed as the thickness of the film increases. Consequently, the transparency of the thin films diminishes. The obtained bandgap decreased as the thickness of the films increased, as indicated in Table I.

Electrical Properties

To evaluate the electrical characteristics, two electrodes were fashioned on the samples using silver paste, facilitating current analysis. The linear increase in current observed with increasing voltage indicated the ohmic nature of the prepared films. These findings are visually depicted in Figs. 3 and 4, illustrating the changes in resistivity and conductivity of tin-doped copper oxide (CuO) thin films as a function of varying thickness. In terms of the calculated resistivity and conductivity, the sample 0.75MD1, with a thickness of 165 nm, exhibited the highest resistivity at 11.86 Ω·m, while the sample 0.75MD4, with a thickness of 570 nm, demonstrated the lowest resistivity at 6.04 Ω·m. Notably, the conductivity of the CuO thin films displayed an upward trend with increasing thickness. As the thickness increased up to 570 nm, the conductivity increased. Our results are consistent with those reported by Visalakshi et al.[33] This phenomenon can be attributed to the increased presence of charge carriers as thickness increases. This increase in charge carriers leads to reduced resistivity, resulting in increased conductivity, as observed. The obtained results are consistent with findings reported previously.[34,35]

Sensitivity

Fabrication of Gas Sensor

To analyze the sensitivity of the Sn-doped CuO thin films toward H_2S gas, a gas sensor was constructed with a stainless-steel homemade test chamber using a digital picoammeter (SES Instruments Pvt. Ltd., Roorkee, model DPM-111) and high-voltage power supply (model EHT-11A). The experimental setup for the gas sensor is shown in Fig. 5.

A PID-controlled oven in the range of 25–200°C was used to control the operating temperature. Two electrodes (1 cm apart) were constructed on each thin film sample using silver paint. H_2S gas in a concentration range of 10–40 ppm was injected using a syringe. To measure the gas response at different operating temperatures (25–100°C), the resistance of each sample was noted before and after exposure to the sensing gas.

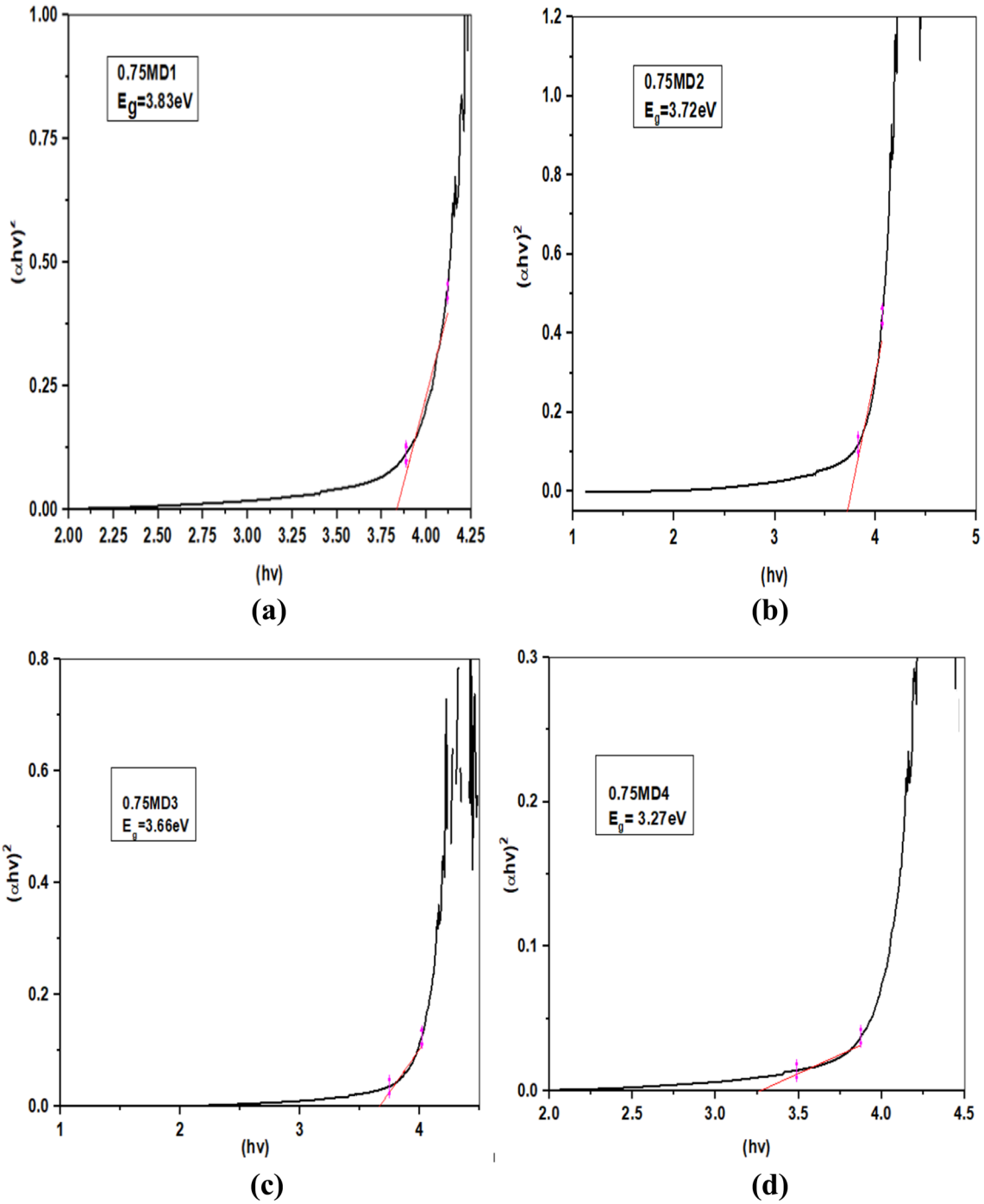

Fig. 2 Bandgaps of samples (a) 0.75MD1, (b) 0.75MD2, (c) 0.75MD3 and (d) 0.75MD4 of CuO doped with 3% Sn.

Mechanism of Gas Sensor

The sensitivity of the prepared CuO films for H_2S gas was investigated at different operating temperatures (25°C, 50°C, 75°C. and 100)°C and concentrations (10–40 ppm). The sensing mechanism of CuO films is based on the change in electrical resistivity and conductivity on exposure to H_2S gas.[36] When this gas is injected, it then interacts with the adsorbed oxygen at the sensor surface, which can be explained by the following reaction:

$$R + O - (\text{ads}) \rightarrow RO + e-, \quad (5)$$

Table I Optical bandgap for samples with varying thicknesses

Name of sample	Thickness (nm)	Optical bandgap (eV)
0.75MD1	165	3.83
0.75MD2	337	3.72
0.75MD3	461	3.66
0.75MD4	570	3.27

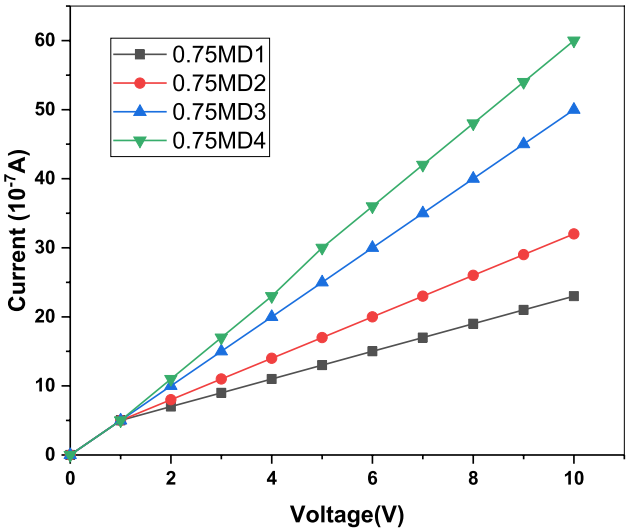

Fig. 3 *I–V* characteristics of Sn-doped CuO thin films.

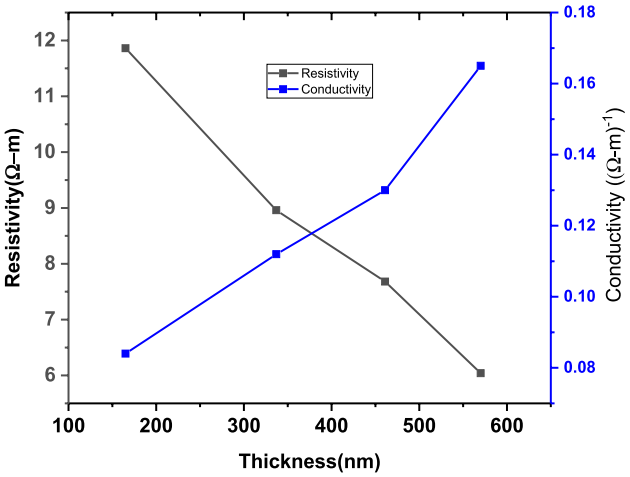

Fig. 4 Variation in resistivity and conductivity of Sn-doped CuO thin films as a function of varying thickness.

where R is the reducing gas, O− (ads) is the oxygen ion adsorption, and e− represents freed electrons.[37,38] The CuO/$SnCl_2$ thin film provides a larger surface area to adsorb and

Fig. 5 Experimental setup of thin film gas sensor for measuring response toward H_2S gas.

diffuse the gas molecules. Figure 6a shows that the *p*-CuO/*n*-SnO_2 interface will form a charge carrier depletion layer, which causes high resistance of sensing materials in air. When H_2S gas is present, the *p–n* junction breaks down due to the transformation of CuO to CuS. Due to this junction breakdown, the depletion layer become thin and the sensing materials exhibit lower resistance, as shown in Fig. 6b.

The response of a film toward hydrogen sulfide gas is defined as follows:

$$\text{Response} = R_a/R_g, \tag{6}$$

where R_a is the air resistance and R_g is the resistance of the exposed gas.

It was found that the response increased as the concentration of the target gas increased. These outcomes closely match those of Jundale et al.[39] This occurs due to decreased resistance on exposing H_2S gas, allowing more current to pass. The gas response is shown by Fig. 7a, b, c, and d. It can be seen that the highest gas response was achieved for the prepared sample with thickness of 165 nm and the lowest response for the sample with thickness of 570 nm. The value of the response decreases because of the decreasing air resistance of the films. It was observed that the response of the films also decreases as the operating temperature increases, which is explained by the oxygen adsorption and desorption phenomenon. These results are in close agreement with those of previous reports.[40–42]

CuO, in the pure form, is reported to show a reversible response toward small concentrations of H_2S, but at low operating temperature (room temperature), CuO is irreversibly converted to CuS, and the sensor loses its response.[12,43,44] However, our thin film samples show better performance characteristics than others at low temperature (Table II).

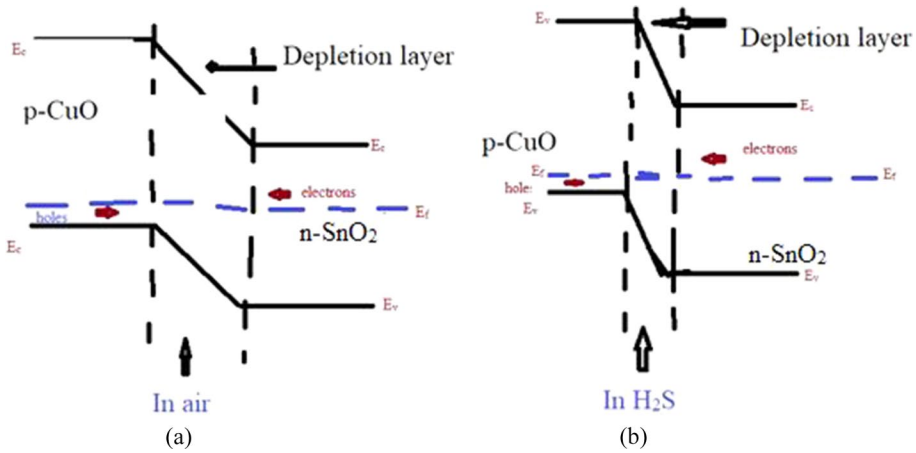

Fig. 6 (a) and (b) The mechanism of the gas sensor.

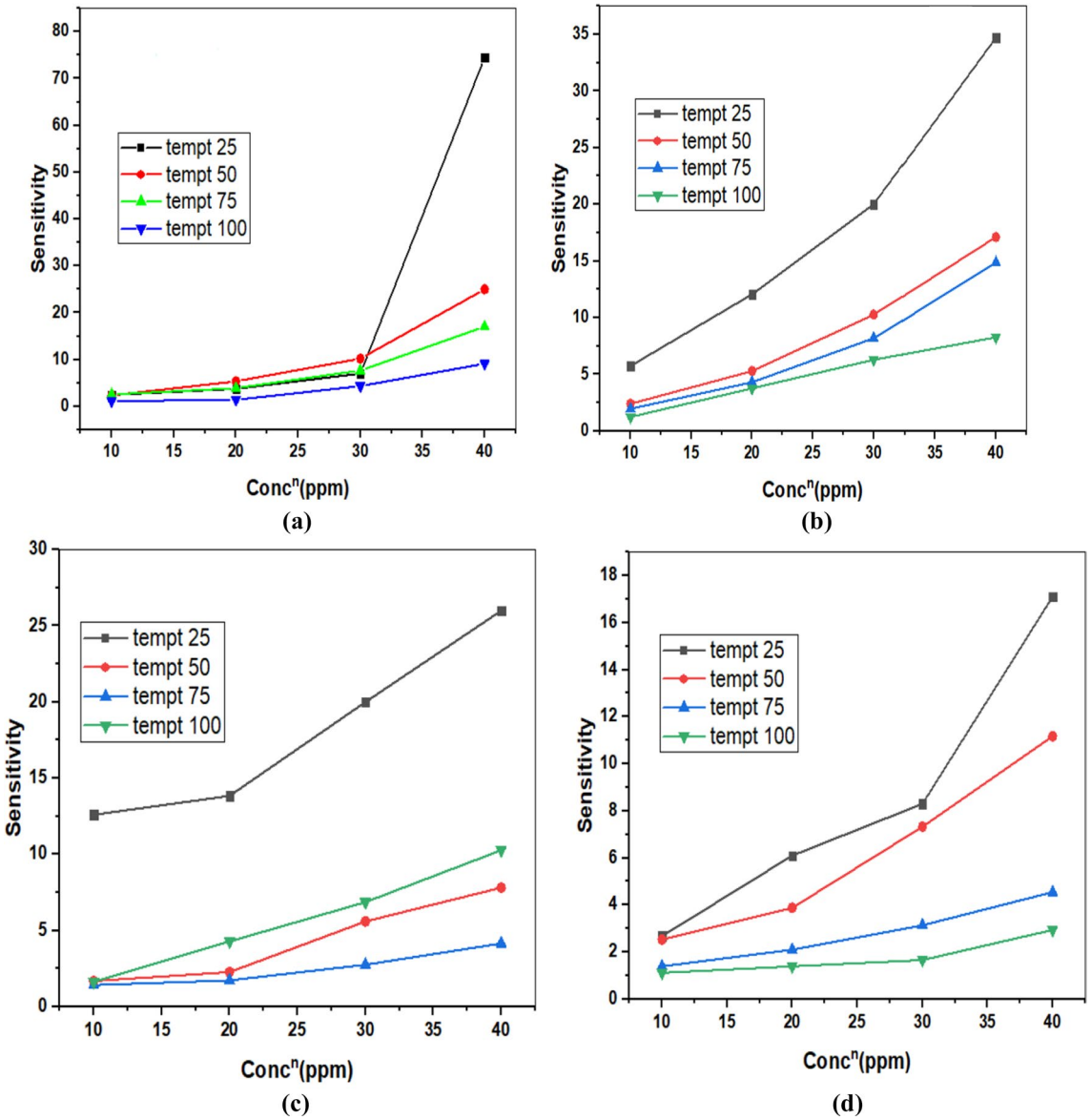

Fig. 7 Gas response for samples (a) 0.75MD1, (b) 0.75MD2, (c) 0.75MD3, and (d) 0.75MD4 with varying gas concentration and operating temperature.

Table II The sensing response of the CuO film for H_2S gas in comparison with sensors reported in the literature

Sensing material	Form	Methodology	Conc^n (ppm)	Operating temperature (°C)	Response	R_t (s)	R_c (s)	Ref.
CuO-SnO_2	Thick films	Precipitation and drop coating	50	150	6.7	30	2400	45
CuO	Nanobelts	Wet chemical	10	135	4.7	28	80	46
Pure CuO	Microsphere	Facile two-step method	10	80	4.4	–	–	47
CuO/$CuFe_2O_4$			10	120	44.8	196	> 3000 (20% recovery)	
ZnO/CuO	Nanorods	Spray pyrolysis and chemical bath method	20	50	21%	122	Could not recover	48
ZnO/CuO	Nanorods	Two-stage solution process	100	100	42	120	120 (70% recovery)	49
Pristine CuO	Nanoparticles	Microwave-assisted method	5	100	7	45	900	50
CuO/WO_3	Thin films	Electron beam evaporation	150	300	30	10	750	51
CNT/SnO_2/CuO	Composite films	Sol–gel spin coating	40	RT	4.41	24	60	52
Sn-doped CuO	Thin films	Sol–gel spin coating	40	RT	74.5	5	160	This work

The H_2S sensing properties of the samples were measured repeatedly over a period of 1-3 years at different temperatures and gas concentrations and found to be highly stable.

Conclusion

Tin-doped copper oxide (CuO) thin films were fabricated using a sol–gel spin-coating technique, and served as a gas-sensing material for hydrogen sulfide (H_2S) detection. The synthesized films were crystallized through annealing at 400°C for 2 h. The electrical conductivity observed spanned from 0.08 Ω^{-1}-m^{-1} to 0.165 Ω^{-1}-m^{-1}. The incorporation of Sn led to the creation of a *p–n* heterojunction, resulting in reduced conductivity. Notably, the introduction of Sn into the semiconducting CuO facilitated effective H_2S response, transforming the semiconducting CuO into conductive copper sulfide (CuS). Sensor responses to different H_2S concentrations were recorded at varying operating temperatures. The best response occurred at 25°C. As the operating temperatures increased, the response diminished due to the adsorption and desorption of oxygen, influencing the film's interaction with the gas.

Acknowledgments We would like to thank the central instrumentation facility in Lovely Professional University, Phagwara, for carrying out characterization of my samples.

Author Contributions Jyoti: preparation of thin films using spin coater, characterization, sensor fabrication, H_2S gas, writing of manuscript, result analysis using software (Origin). Rajesh Kumar and Ashok Kumar: supervision, editing of manuscript.

Data Availability The information was gathered through experimentation, with additional materials provided by the institution.

Conflict of interest The authors declare that they are not aware of any personal or financial conflicts that might have appeared to affect the research reported in this study.

References

1. N.M. Vuong, N.D. Chinh, B.T. Huy, and Y.I. Lee, CuO-decorated ZnO hierarchical nanostructures as efficient and established sensing materials for H_2S gas sensors. *Sci. Rep.* 6, 26736 (2016).
2. Z. Guo, G. Chen, G. Zeng, L. Liu, and C. Zhang, Metal oxides and metal salt nano structures for hydrogen sulfide sensing: mechanism and sensing performance. *RSC Adv.* 5, 54793 (2015).
3. H. Sawalha, M. Maghalseh, J. Qutaina, K. Junaidi, and E.R. Rene, Removal of hydrogen sulfide from biogas using activated carbon synthesized from different locally available biomass wastes: a case study from Palestine. *Bioengineered* 11(1), 607 (2020).
4. M.J. Priya, P.P. Subha, P.M. Aswathy, K.W. Merin, M.K. Jayaraj, and K.R. Kumar, Selective detection of hydrogen sulphide from the background of low concentration reducing gases. *Mater. Chem. Phys.* 260, 124038 (2021).
5. Y. Guo, M. Gong, Y. Li, Y. Liu, and X., Dou sensitive, selective, and fast detection of ppb-level H_2S gas boosted by ZnO-CuO mesocrystal. *Nanoscale Res. Lett.* (2016). https://doi.org/10.1186/s11671-016-1688-y.
6. G.A. Poda, Hydrogen sulfide can be handled safely. *Arch. Env. Health.* 12(6), 795 (1966).
7. H. Li, W. Sun, X. Yu, L. Du, and M. Li, Coumarin-based fluorescent probes for H_2S detection. *J. Fluoresc. Fluoresc.* 23, 181 (2013).
8. M. Hanada, H. Koda, K. Onaga, K. Tanaka, T. Okabayashi, T. Itoh, and H. Miyazaki, Portable oral malodor analyzer using

highly sensitive In_2O_3 gas sensor combined with a simple gas chromatography system. *Anal. Chim. Acta* 475, 27–35 (2003).
9. H.A. Henthorn and M.D. Pluth, Mechanistic insights into the H_2S-mediated reduction of aryl azides commonly used in H_2S detection. *J. Am. Chem. Soc.* 135, 15330 (2015).
10. V. Khoramshahi, M. Azarang, M. Nouri, A. Shirmardi, and R. Yousefi, Metal oxide/g-C_3N_4 nanocomposites chemiresistive gas sensors: a review on enhanced performance. *Tal. Open.* 9, 80 (2024).
11. N.S.A. Eom, H.B. Cho, Y. Song, G.M. Go, J. Lee, and Y.H. Choa, Room-temperature H_2S gas sensing by selectively synthesized $Cu_{x(x=1,2)}O$:SnO_2 thin film nanocomposites with oblique & vertically assembled SnO_2 ceramic nanorods. *Sens. Actuat. B Chem.* 273, 1054 (2018).
12. M. He, L. Xie, X. Zhao, X. Hu, S. Li, and Z.G. Zhu, Highly sensitive and selective H_2S gas sensors based on flower-like WO_3/CuO composites operating at low/room temperature. *J. Alloys Compd.* 788, 36 (2019).
13. B. Urasinska-Wojcik, T.A. Vincent, and J.W. Gardner, H_2S sensing properties of WO_3 based gas sensor. *Proc. Eng.* 168, 255 (2016).
14. C. Zhang, K. Xu, K. Liu, J. Xu, and Z. Zheng, Metal oxide resistive sensors for carbon dioxide detection. *Coord. Chem. Rev.* 472, 214758 (2022).
15. S. Liu, W. Yang, L. Liu, H. Chen, and Y. Liu, Enhanced H_2S gas-sensing performance of Ni-doped ZnO nanowire arrays. *ACS Omega* 8, 7595 (2023).
16. P.G. Choui, T. Fuchigami, K. Kakimoto, and Y. Masuda, Effect of crystal defect on gas sensing properties of Co_3O_4 nanoparticles. *ACS Sens.* 5, 1662 (2020).
17. D. Jung, S. Hwang, H.J. Kim, J.H. Han, and H.-N. Lee, Characterization of porous CuO films for H_2S gas sensors. *Materials* 15, 7220 (2022).
18. A.K. Gangwar, R. Godiwal, S. Srivastava, P. Pal, G. Gupta, and P. Singh, Preparation of nanocrystalline Pd/SnO_2 thin films deposited on alumina substrate by reactive magnetron sputtering for efficient CO gas sensing. *Mater. Res. Bull.* 148, 111692 (2020).
19. D. Nagmani, A. Pravarthana, T.C. Tyagi, W. Jagadale, and D.K. Prellier, Aswal, highly sensitive and selective H_2S gas sensor based on TiO_2 thin films. *Appl. Surf. Sci.* 549, 49281 (2021).
20. G. Ramanathan, N. Srinivasan, and K.R. Murali, Detection of H_2S gas sensing performance of sol gel prepared metal oxide (In_2O_3, SnO_2, Sn doped In_2O_3) thin films. *Mater. Today: Proc.* 92, 1218 (2023).
21. R.K. Jain and A. Khanna, CuO-doped WO_3 thin film H_2S sensors. *Sens. Actuat. B: Chem.* 343, 130153 (2021).
22. S. Steinhauer, Gas sensors based on copper oxide nanomaterials: a review. *Chemosensors* 9, 51 (2021).
23. S. Werner, C. Glaser, T. Kasper, T.N. Nguyên, S. Gross, and B.M. Smarsly, H_2S dosimetry by CuO: towards stable sensors by unravelling the underlying solid-state chemistry. *Chem.: A Eur. J.* 28, 2 (2021).
24. F. Peng, Y. Sun, W. Yu, Y. Lu, J. Hao, R. Cong, M. Ge, J. Shi, and N. Dai, Studies on sensing properties and mechanism of CuO nanoparticles to H_2S gas. *Nanomaterials* 10, 1 (2020).
25. J. Deng and Z.Y. Zhao, Effects of non-stoichiometry on electronic structure of Cu_xS_y compounds studied by first-principle calculations. *Mater. Res. Express* 6, 105513 (2019).
26. B.D. Cullity, *Elements of X-Ray Diffraction* (Reading: Addison-Wesley Publishing Company, 1978).
27. E.R. Shaaban, N. Afify, and A. El-Taher, Effect of film thickness on microstructure parameters and optical constants of CdTe thin films. *J. Alloys Compd.* 482, 400 (2009).
28. A. Prakash, V. Mishra, and M.G. Mahesh, Development of enduring interstitial defects in Mg-doped CuO thin films. *RSC Adv.* 14, 10004 (2024).
29. M. Ajili, S. Dabbabi, N. Bouarissia, and T.N. Kamoun, Investigation on substrate effect on physical characteristics of CuO-sprayed thin films suitable for photovoltaic application: Ag/ZnO: Sn (n)/CuO (p)/Sn_O2:F. *Sol. Ene. Mater. Technol.* 37, 381 (2020).
30. S. Chackrabarti, S.A. Bhat, B.M.U.D. Bhat, I. Khan, and R.A. Zargar, Investigation on the structural and optical properties of Zn_{1-x} Cu_xO (x = 0, 0.05, 0.1) sintered films for optoelectronic device applications. *Eur. Chem. Bull.* 6(10), 426 (2017).
31. R.D. Tarey and T.A. Raju, A method for the deposition of transparent conducting thin films of tin oxide. *Thin Soli. Film* 128, 181 (1985).
32. X.L. Zhang, K.S. Hui, F. Bin, K.N. Hui, L. Li, Y.R. Cho, R.S. Mane, and W. Zhou, Effect of thermal annealing on the structural, electrical and optical properties of Al-Ni co-doped ZnO thin films prepared using a sol–gel method. *Surf. Coat. Tech.* 261, 149 (2015).
33. S. Visalakshi, R. Kannan, S. Valanarasu, A. Kathalingam, and S. Rajashabala, Studies on optical and electrical properties of SILAR-deposited CuO thin films. *Ene. Mat.* 21(3), 146 (2016).
34. S.S. Shariffudin, S.S. Khalid, N.M. Sahat, M.S.P. Sarah, and H. Hashim, Preparation and characterization of nanostructured CuO thin films using sol–gel dip coating. *IOP Conf. Series: Mater. Sci. Eng.* 99, 012007 (2015).
35. J. Wu, K.S. Hui, K.N. Hui, L. Li, H.H. Chun, and Y.R. Cho, Characterization of Sn-doped CuO thin films prepared by sol–gel method. *J. Mater. Sci. Mater. Electron.* 27, 1719 (2015).
36. P. Shankar and J.B.B. Rayappan, Gas sensing mechanism of metal oxides: the role of ambient atmosphere, type of semiconductor and gases: a review. *Sci. Lett. J.* 4, 126 (2015).
37. F.-N. Meng, X.-P. Di, H.-W. Dong, Y. Zhang, C.-L. Zhu, C. Li, and Y.-J. Chen, Ppb H_2S gas sensing characteristics of Cu_2O/CuO sub-microspheres at low-temperature. *Sensor. Actuator. B Chem.* 182, 197 (2013).
38. A.I. Ayesh, A.A. Alyafei, R.S. Anjum, R.M. Mohamed, M.B. Abuharb, B. Salah, and M. El-Muraikhi, Production of sensitive gas sensors using CuO/SnO_2 nanoparticles. *Appl. Phys. A Mater. Sci. Process.* 125, 1 (2019).
39. D. Jundale, S. Pawar, M. Chougule, P. Godse, S. Patil, B. Raut, S. Sen, and V. Patil, Nanocrystalline CuO thin films for H_2S monitoring: microstructural and optoelectronic characterization. *J. Sens. Tech.* 1, 36 (2011).
40. F.I.M. Ali, S.T. Mahmoud, F. Awwad, Y.E. Greish, and A.F.S. Abu-Hani, Low power consumption and fast response H_2S gas sensor based on a chitosan-CuO hybrid nanocomposite thin film. *Carb. Poly.* 236, 116064 (2020).
41. C. Fan, F. Sun, X. Wang, M. Majidi, Z. Huang, P. Kumar, and B. Liu, Enhanced H_2S gas sensing properties by the optimization of *p*-CuO/*n*-ZnO composite nanofibers. *J. Mater. Sci.* 55, 7702–7714 (2020).
42. A. Kumar, A.K. Shringi, and M. Kumar, RF sputtered CuO anchored SnO_2 for H_2S gas sensor. *Sens. Actua. B: Chem.* 370, 132417 (2022).
43. A. Khanna, R. Kumar, and S.S. Bhatti, CuO-doped SnO_2 thin films as hydrogen sulfide gas sensor. *Appl. Phys. Lett.* 82, 4388 (2003).
44. N.S. Ramgir, S.K. Ganapathi, M. Kaur, N. Datta, K.P. Muthe, D.K. Aswal, S.K. Gupta, and J.V. Yakhmi, Sub-ppm H_2S sensing at room temperature using CuO thin films. *Sens. Actuat. B Chem.* 151, 90 (2010).
45. J. Liu, X. Huang, G. Ye, W. Liu, Z. Jiao, W. Chao, Z. Zhou, and Z. Yu, H_2S Detection sensing characteristic of CuO/SnO_2 sensor. *Sensors.* 3, 110 (2003).
46. Y.-J. Chen, F.-N. Meng, H. Yu, C. Zhu, T. Wang, P. Gao, and Q. Ouyang, Sono-chemical synthesis and ppb H_2S sensing performances of CuO nanobelts. *Sens. Actuat. B Chem.* 176, 15 (2013).

47. X. Hu, Z. Zhu, Z. Li, L. Xie, Y. Wu, and L. Zheng, Heterostructure of CuO microspheres modified with $CuFe_2O_4$ nanoparticles for highly sensitive H_2S gas sensor. *Sens. Actuat. B Chem.* 264, 139 (2018).
48. D. Li, L. Qin, P. Zhao, Y. Zhang, D. Liu, F. Liu, B. Kang, Y. Wang, H. Song, T. Zhang, and G. Lu, Preparation and gas-sensing performances of ZnO/CuO rough nanotubular arrays for low-working temperature H_2S detection. *Sens. Actuat. B Chem.* 254, 834 (2018).
49. L. Wang, Y. Kang, Y. Wang, B. Zhu, S. Zhang, W. Huang, and S. Wang, CuO nanoparticle decorated ZnO nanorod sensor for low-temperature H_2S detection. *Mater. Sci. Eng. C* 32, 2079 (2012).
50. L. Yin, H. Wang, L. Li, H. Li, D. Chen, and R. Zhang, Microwave-assisted preparation of hierarchical CuO@rGO nanostructures and their enhanced low-temperature H_2Ssensing performance. *Appl. Surf. Sci.* 476, 107 (2019).
51. R.K. Jain and A. Khanna, CuO-doped WO_3 thin film H_2S sensors. *Sens. Actuat. B Chem.* 343, 130153 (2021).
52. Y. Zhao, J. Zhang, Y. Wang, and Z. Chen, A highly sensitive and room temperature CNTs/SnO_2/CuO sensor for H_2S gas sensing applications. *Nanoscale Res. Lett.* 15(40), 3 (2020).